Research Article **Open Access**

Alberto Carpinteri, Giuseppe Lacidogna*, and Giuseppe Nitti

Open and closed shear-walls in high-rise structural systems: Static and dynamic analysis

DOI 10.1515/cls-2016-0013
Received Apr 26, 2016; accepted Apr 28, 2016

Abstract: In the present paper, a General Algorithm is applied to the analysis of high-rise structures. This algorithm is to be used as a calculation tool in preliminary design; it allows to define the interaction between closed and open, straight or curved shear-walls, and the forces exchanged in structures subject to mainly horizontal loads. The analysis can be performed in both static and dynamic regimes, the mode shapes and the natural frequencies being assessed. This general formulation allows analyses of high-rise structures by taking into account the torsional rigidity and the warping deformations of the elements composing the building without gross simplifications. In this way it is possible to model the structure as a single equivalent cantilever, thus minimising the degrees of freedom of the system, and consequently the calculation time.
Finally, potentials of the method proposed are demonstrated by a numerical example which emphasizes the link between global displacements and stresses in the elements composing the structure.

Keywords: Open-sections; Vlasov's theory; Structural Systems; Structural behaviour; Tall buildings

1 Introduction

In the field of Structural Mechanics, the conventional theory of de Saint Venant shows some limits in analyzing the so-called thin-walled beams. This is due to the fact that the elastic theory on the three-dimensional beam is based on the hypothesis of a "compact" transversal section: the average size of the section should be comparable to the thickness of each component element. As the compact section hypothesis is not acceptable in case of thin-walled beams, new theories were needed, the "higher-order theories", that are valid beyond Saint Venant's hypotheses.

An elastic theory for thin-walled beams was developed in the years between the two world wars and is known as the theory of sectorial areas. An almost final version was defined by Vlasov [1] and this theory is often named after him, even if it was based on independent proposals by other authors [2–4]. Capurso [5] subsequently presented refined details for the method of application of external actions and the influence of constraints on section warping. The same author also extended the theory of thin-walled beams to tall buildings stiffened by open and closed shear-walls and loaded by transverse actions applied to the floor planes [6].

The objective of this paper is to present an approximate method for the efficient design of thin-walled open-sections in tall buildings. The method is simple, inexpensive, and provides the designer with accurate results for all the necessary design parameters, *e.g.*, bending and torsional stresses in the open and closed shear-walls and the displacements (lateral and torsional) through the height of the structure. To achieve this goal, a General Algorithm originally proposed in [7] is employed. On the basis of this approach, the General Algorithm is extended to encompass any combination of bracings, including bracings with thin-walled open-sections, which are analyzed in the framework of Timoshenko-Vlasov theory [1, 8] of sectorial areas and according to the approach by Capurso [6].

Tall buildings are one of the representation of the technological progress of nations. In most of cases, tall buildings are the symbol of the town, such as Empire State Building in New York, Willis Tower in Chicago, Petronas Towers in Kuala Lumpur, Burj Khalifa in Dubai, and so on. In accordance with population growth in the towns, tall buildings are being developed in particular areas of the planet. The Home Insurance Building of Chicago is generally considered as the first tall building, opened in 1884, has 12 storeys to a height of 42 m. Until the middle of the 20th century, the urban landscape represented by tall buildings was a prerogative of New York, Chicago, Houston and some other United States cities. The tallest build-

Alberto Carpinteri, Giuseppe Nitti: Department of Structural, Geotechnical and Building Engineering (DISEG), Politecnico di Torino, Torino, Italy
***Corresponding Author: Giuseppe Lacidogna:** Department of Structural, Geotechnical and Building Engineering (DISEG), Politecnico di Torino, Torino, Italy; Email: giuseppe.lacidogna@polito.it

ing of the world, until 1997, was the Sears Tower (442 m) in Chicago. This record was yielded at the Petronas Towers (452 m) in Kuala Lumpur and for the first time the record of the tallest building comes out from the United States.

In 2004, Taipei 101 in Taipei surpassed the Petronas Towers by soaring to a height of 509 m to become the world's tallest building. It retained the title until Burj Khalifa was completed in 2010, which rises to 828 m. Nowadays, most of the super-tall buildings are located far from the United States: China, Korea, Malaysia, Saudi Arabia, United Arab Emirates and other emerging countries characterized by a considerable economic capability and technological progress, represent an evident proof of this current trend. The spread of computers and technological progress facilitated the development of new forms and structural systems.

The choice of the structural system has a great importance to decrease the effective cost of tall buildings. In the constructions, the main function of the structural system is to carry gravity loads. On the other hand, gradually increasing the structural height, its function was improved to include resistance against horizontal forces. For tall buildings, horizontal forces are principal load case in the design of the structural system. A critical parameter for structural efficiency is the building's slenderness ratio (ratio of height to minimum width). Slender towers require special measures to counteract the wind forces. These can include additional parts to stiffen the building. Today there are different lateral bracing systems, and they may be grouped into distinct categories, each one with an applicable height range [9]. However, the effective stiffness of lateral load resisting systems typically includes one or a combination of the different systems. In the following the approximate number of stories requiring the corresponding system is listed.

1. Frames with semi-rigid connections (10–15 storeys);
2. Rigid frames (not exceeding 25 storeys);
3. Braced frames (25–30 storeys);
4. Framed tube (50–60 storeys);
5. Trussed tube (60–70 storeys);
6. Bundled tube (80–100 storeys).

The structural analysis of this kind of structures can be done using finite element (FE) programmes. However, as observed by many authors including Howson [10], Steenbergen and Blaauwendraad [11], these models have their deficiency. Even using powerful computers, the modelling is usually very difficult, consequently the long time of calculation leading to high budgets. The complexity of the results can lead to errors of perception or to lack of understanding of the mechanics of the structure and its structural response. Furthermore, by performing FE analysis, it is difficult to understand the interaction between the macro-structural elements concealed behind the great number of input and output data. As remarked by Howson [10], the use of FE models is universally accepted for the final design but the use of this type of models at an early or preliminary design stage can be not only time-consuming but also unproductive. Simplified procedures based on carefully chosen approximations represent the possible alternative for the analysis. A simplified global model can offer many potential benefits including easy input, quick input processing, and clear, simple and direct results performance.

Furthermore the modelling procedures are likely to be simpler, thus, less prone to be a potential source of error; instead the accuracy, although not as high as in FE simulations, is sufficient for the preliminary design stage. The first models, developed in the 1960s and 1970s, addressed the case of shear-wall frame interaction; among them, we could cite the analytical approaches by Khan and Sbarounis [12], Coull and Irwin [13], Heidebrecht and Stafford Smith [14], Rutenberg and Heidebrecht [15], and Mortelmans *et al.* [16]. In all these models, the entire structure is idealized as a single shear-flexural equivalent cantilever. However, only one degree of freedom (DOF) per storey is considered, and the torsional and flexural problems are separated treated. Similar models have also been developed for three-dimensional structures, in particular for framed-tube structures, as described by Khan [17], Coull and Bose [18], Connor *et al.* [19], Kwan [20], and Rahgozar *et al.* [21] among others. Moreover, other simplified methods can be applied in cases where the vertical stiffening structures are constituted by frames [22, 23], or by open shear walls [24]. In the literature there are also simplified methods for the dynamic analysis of tall buildings that involve the use of analytical [25, 26] or FE models [27].

The main problem with all these simplified models is the lack of generality, as the same formulation often cannot be used to analyze buildings with different underlying structural typologies. A first attempt to formulate a General Algorithm is due to the work of Carpinteri and Carpinteri [7].

As previously said, by the extension of the General Algorithm it is possible to define the interaction between closed and open cores within the same structure and what are the forces exchanged. In this context there are the tall buildings in which are often found resistant elements of various nature, *e.g.* open and closed shear-wall, straight or curved shear wall, frames and so on, due to current architectural trends which lead to complex shapes. By using the General Algorithm, some papers about the problem

of the structural analysis of tall buildings under horizontal load have been published by two of the authors of this work in international journals [28–32]; the studies involve both nonexisting and real buildings.

In Section 2 is summarized the original approach by Carpinteri [7], in Section 3 is condensed the Vlasov's theory [1] for thin-walled open-section beams and their interaction in the structures (Capurso's Method [6]). Section 4 draws attention to the problem of dynamic analysis, calculates the frequencies of vibration and modal shapes, while Section 5 presents a numerical example showing the effectiveness and flexibility of the combined approach.

2 Carpinteri's General Algorithm

The general formulation of the problem of the external lateral loading distribution between the bracings of a three-dimensional structure, was presented in 1985 by Carpinteri and Carpinteri [7], will be revisited in this Section. These are cantilevers often characterised by thin-walled open sections which allow to house stairwells and/or lift shafts. The structure consisting of M bracings interconnected through undeformable storey in their planes, and the axial deformations of bracings are not considered. Since the slabs, which interconnect the bracings to each other, are considered to be infinitely rigid in their own planes, the degrees of freedom are represented by the transverse displacements of the single floors: two translations ξ and η in the directions X and Y, and the torsional rotation ϑ, for each storey.

The analysis of this composed system is primarily focused on the identification of the distribution of external forces among the single components. The formulation is based on the following fundamental hypotheses:

(i) the structural material is homogeneous, isotropic, and obeys Hooke's law;
(ii) the floor slabs are rigid in their own plane but their out-of-plane rigidity is negligible;
(iii) in the transversal analysis, the axial deformation of the structural elements due to gravity loads is neglected.

The approach proves to be general, since it is possible to consider any type of vertical bracing, from simple frames to free-shaped tubular elements, provided that their own stiffness matrix is known.

Based on the previously mentioned hypotheses, the building have $3N$ degrees of freedom, in the same way, the external load applied to the origin of the reference system is expressed by a $3N$-vector $\{F\}$, in which $2N$ shearing forces $\{p_x\}$, $\{p_y\}$ and N torsional moments $\{m_z\}$ are included (Figure 1):

$$\{F_i\} = \begin{Bmatrix} p_i \\ m_{z,i} \end{Bmatrix} = \begin{Bmatrix} p_{x,i} \\ p_{y,i} \\ m_{z,i} \end{Bmatrix} \tag{1}$$

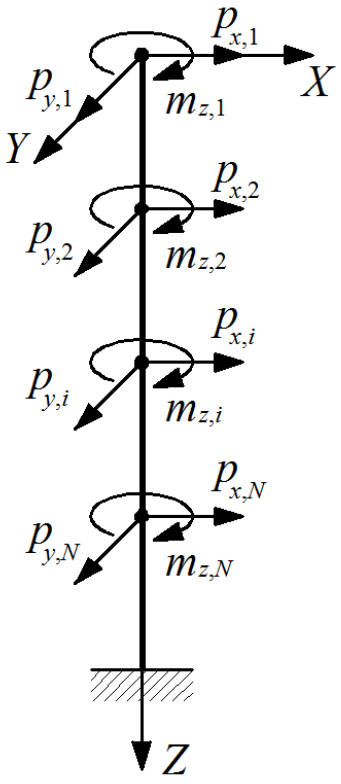

Figure 1: Scheme of a tall building in a right-handed coordinate system.

Being the right-handed system $X_i^\star Y_i^\star Z_i^\star$ the local coordinate system of the i-th bracing, the $3N$-load vector $\{F_i^\star\}$ and the $3N$-displacement vector $\{\delta_i^\star\}$ describe the amount of external load carried by the i-th element and its transverse displacements, respectively.

The loading vector $\{F_i^\star\}$ can be reduced to $\{F_i\}$, which refers to the global coordinate system XYZ, by means of the following expressions, valid for each floor:

$$\begin{Bmatrix} p_{x,i}^\star \\ p_{y,i}^\star \\ m_{z,i}^\star \end{Bmatrix} = \begin{bmatrix} [N_i] & [0] \\ -\{u_z\} \wedge \{\psi_i\} & [1] \end{bmatrix} \begin{Bmatrix} p_{x,i} \\ p_{y,i} \\ m_{z,i} \end{Bmatrix} \tag{2}$$

where [1] is the identity matrix and [0] is the null matrix.

The term $[N_i]$ represents the orthogonal rotation matrix from system XY to system $X_i^\star Y_i^\star$; $\{\psi_i\}$ is the coordinate

vector of the origin of the local system in the global one; $\{u_z\}$ is the unit vector associated to the Z direction. The orthogonal matrix $[N_i]$, extended to consider all floors, can be represented by means of the angle φ_i between Y and $Y_i^\star$ axes (Figure 2):

$$[N_i] = \begin{bmatrix} [\cos\varphi_i] & [\sin\varphi_i] \\ -[\sin\varphi_i] & [\cos\varphi_i] \end{bmatrix} \tag{3}$$

where each term is a diagonal $N \times N$ sub-matrix:

$$[\cos\varphi_i] = \begin{bmatrix} \cos\varphi_i & 0 & \cdots & 0 \\ 0 & \cos\varphi_i & \cdots & 0 \\ \vdots & \vdots & & \vdots \\ 0 & 0 & \cdots & \cos\varphi_i \end{bmatrix} \tag{4a}$$

$$[\sin\varphi_i] = \begin{bmatrix} \sin\varphi_i & 0 & \cdots & 0 \\ 0 & \sin\varphi_i & \cdots & 0 \\ \vdots & \vdots & & \vdots \\ 0 & 0 & \cdots & \sin\varphi_i \end{bmatrix} \tag{4b}$$

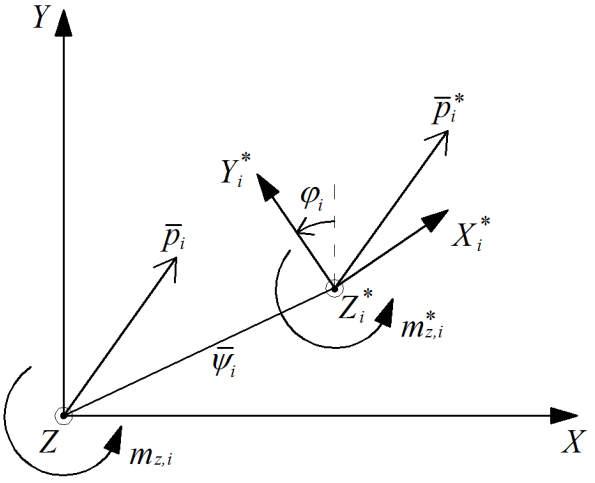

Figure 2: Global and local coordinate systems.

For the sake of simplicity, in order to take into account the N floors of the structure, this vector product can be written as a $2N \times N$ matrix $[C_i]$ composed by two diagonal sub-matrices containing the coordinates $(x_i; y_i)$ of the origin of the local system $X_i^\star Y_i^\star$:

$$-\{u_z\} \wedge \{\psi_i\} = -\begin{vmatrix} \bar{i} & \bar{j} & \bar{k} \\ 0 & 0 & 1 \\ x_i & y_i & 0 \end{vmatrix} = -\begin{bmatrix} -y_i & x_i \end{bmatrix} = -[C_i]^T \tag{5}$$

Taking into account all floors, Equation (2) can be rewritten in the following form:

$$\left\{F_i^\star\right\} = [A_i]\{F_i\} \tag{6}$$

Matrix $[A_i]$ gathers the information regarding the reciprocal rotation between the local and global coordinate systems and the location of the i-th bracing in the global system XY:

$$[A_i] = \begin{bmatrix} [N_i] & [0] \\ -[C_i]^T & [1] \end{bmatrix} \tag{7}$$

In the same way, the vector $\{\delta_i^\star\}$, constituted by $2N$ translations $\xi_i^\star$, $\eta_i^\star$ and N rotations $\vartheta_i^\star$, can be connected to the corresponding $\{\delta_i\}$, which is referred to the global coordinate system, by means of the compact $3N \times 3N$ matrix $[B_i]$:

$$\left\{\delta_i^\star\right\} = \begin{Bmatrix} \xi_i^\star \\ \eta_i^\star \\ \vartheta_i^\star \end{Bmatrix} \tag{8}$$

The displacements $\{\delta_i\}$ in the global coordinate system XY are then connected to the displacements $\{\delta_i^\star\}$ in the local coordinate system $X_i^\star Y_i^\star$ by the orthogonal matrix $[N_i]$:

$$\begin{Bmatrix} \xi_i^\star \\ \eta_i^\star \\ \vartheta_i^\star \end{Bmatrix} = \begin{bmatrix} [N_i] & [0] \\ [0] & [1] \end{bmatrix} \begin{Bmatrix} \xi_i \\ \eta_i \\ \vartheta_i \end{Bmatrix} \tag{9}$$

Taking into account all floors, Equations (9) can be rewritten in the following form:

$$\left\{\delta_i^\star\right\} = [B_i]\{\delta_i\} \tag{10}$$

where matrix $[B_i]$ is similar to $[A_i]$, the term $[C_i]^T$ being reduced to a null matrix:

$$[B_i] = \begin{bmatrix} [N_i] & [0] \\ [0] & [1] \end{bmatrix} \tag{11}$$

A relation between $\{F_i^\star\}$ and $\{\delta_i^\star\}$ is considered known through the condensed stiffness matrix $[\mathrm{K}_i^\star]$, referred to the local coordinate system:

$$\left\{F_i^\star\right\} = \left[K_i^\star\right]\left\{\delta_i^\star\right\} \tag{12}$$

Substituting Equations (6) and (10) into Equation (12), the load vector $\{F_i\}$ turns out to be connected to the displacement vector $\{\delta_i\}$ through a product of matrices, which identifies the stiffness matrix $[K_i]$ of the i-th bracing in the global coordinate system XY:

$$\{F_i\} = \left([A_i]^{-1}\left[K_i^\star\right][B_i]\right)\{\delta_i\} = [K_i]\{\delta_i\} \tag{13}$$

Due to the presence of in-plane rigid slabs connecting the vertical cantilevers, the transverse displacements of each element can be computed considering only three

generalised displacements ξ, η, and ϑ per floor. This step, extended to consider all floors, is performed through the matrix $[T_i]$, which takes into account the location of each bracing in the plan by means of the coordinates $(x_i; y_i)$ and, therefore, the matrix $[C_i]$:

$$\{\delta_i\} = \begin{bmatrix} [1] & [C_i] \\ [0] & [1] \end{bmatrix} \{\delta\} = [T_i]\{\delta\} \tag{14}$$

being $\{\delta\}$ the floor displacement vector, *i.e.* the displacement vector associated to the origin of the global reference system.

The substitution of Equation (14) into Equation (13) allows to identify the stiffness matrix of the i-th bracing, referred to the global coordinate system XYZ and to the generalised floor displacements ξ, η, and ϑ:

$$\{F_i\} = ([K_i][T_i])\{\delta\} = \left[\overline{K}_i\right]\{\delta\} \tag{15}$$

For the global equilibrium, the external load $\{F\}$ applied to the structure is equal to the sum of the M vectors $\{F_i\}$. In this way a relationship between the external load and the floor displacements is obtained and the global stiffness matrix of the structure is computed. By means of this matrix, once the external load is defined, the displacements of the structure are acquired, from which the information regarding each single bracing can be deduced

$$\{F\} = \sum_{i=1}^{M} \{F_i\} = \left(\sum_{i=1}^{M} \left[\overline{K}_i\right]\right)\{\delta\} = \left[\overline{K}\right]\{\delta\} \tag{16}$$

and, therefore,

$$\{\delta\} = \left[\overline{K}\right]^{-1}\{F\} \tag{17}$$

Recalling Equation (15) and comparing it with Equation (17), an equation connecting the vectors $\{F\}$ and $\{F_i\}$ allows to define the amount of the external load carried by the i-th vertical stiffening element:

$$\{\delta\} = \left[\overline{K}\right]^{-1}\{F\} = \left[\overline{K}_i\right]^{-1}\{F_i\} \tag{18}$$

from which we obtain

$$\{F_i\} = \left[\overline{K}_i\right]\left[\overline{K}\right]^{-1}\{F\} = [R_i]\{F\} \tag{19}$$

The load distribution matrix $[R_i]$, shown in Equation (19), demonstrates that each bracing is subjected to a load $\{F_i\}$ which is connected with the external load $\{F\}$ through its own stiffness matrix and the inverse of the global stiffness matrix.

Once the generalised displacement vector $\{\delta\}$ is known, recalling Equations (8), (12), and (14), the displacements and the forces related to the i-th bracing, in its local coordinate system, can be computed. Consequently, since the loads applied to each element are clearly identified, a preliminary assessment can be easily performed.

Equation (19) solves the problem of the external load distribution between the resistant elements employed to stiffen a three-dimensional tall building. Such formulation proves to be general and can be adopted with any kind of structural elements, provided that their own condensed stiffness matrix $[K_i^*]$ is known.

Further benefits can be highlighted: firstly, an easy identification of the structural parameters, which govern the lateral behaviour of the building, can be performed; secondly, the formulation proves to be extremely clear and concise, limiting in this way the risk of unexpected errors and guaranteeing, in presence of very complex structures, relatively short times of modelling and analysis, if compared to Finite Element computations.

3 Thin-walled open-section beams in torsion: Vlasov's theory

Unlike hollow sections, in presence of torsional actions, thin-walled open-sections elements reveal a particular behaviour, which is far from Saint Venant's results. Once the torsional deformation takes place, the section twists around its shear centre but, at the same time, does not remain plane, since it undergoes different longitudinal extensions causing an out-of-plane distortion, the so-called **warping**, of the section. As a consequence, a further longitudinal stress, absent in the theory of primary torsion, develops in the thickness of the section.

Let us consider the case of a cantilever I-beam subjected to a concentrated load on one of its flanges (Figure 3). Based on the Superposition Principle, this load can be reduced to the sum of four different loading cases: one is purely axial, two are purely flexural; whilst the other

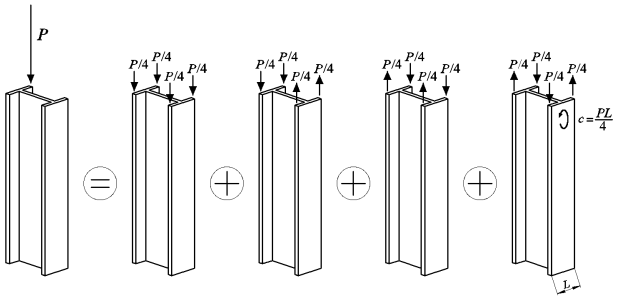

Figure 3: Cantilever I-beam subjected to a concentrated load on one of its flanges.

is defined as flexural torsion, since the two flanges are forced to bend in opposite directions on their own planes. In the latter case, the section does not remain plane and additional normal stresses appear. These additional normal stresses give rise to a generalised action, called **bimoment**, which is directly connected to the warping of the section and consists of two bending moments, each one acting on a single flange, having the same magnitude but opposite signs.

The intensity of this stress state cannot be neglected for these profiles and the application of Saint Venant's theory could lead to gross errors.

Two main geometrical hypotheses are at the basis of Vlasov's theory:

(i) the section is considered rigid and, therefore, its shape is undeformable;
(ii) the shearing strains on the midline of the section are assumed to vanish.

Let us consider a free shaped thin-walled open-section beam, located in a generic coordinate system, in which the Z axis is parallel to the longitudinal axis of the beam. Defined a specific cross section at $z = constant$, X and Y axes complete the right-handed coordinate system XYZ. Each point of the midline can be identified by using the coordinates (x, y) or, along the midline, the curvilinear coordinate s (Figure 4).

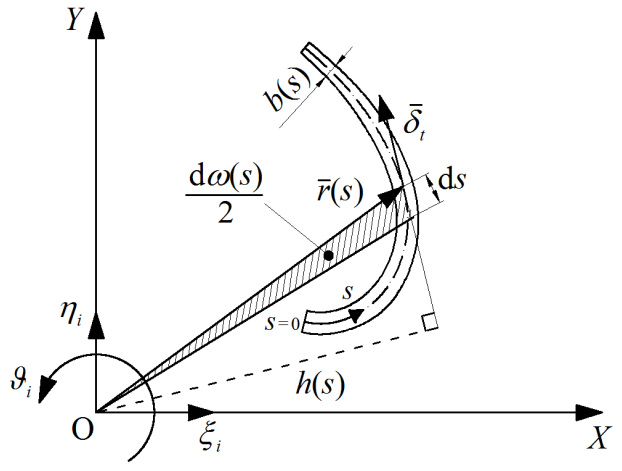

Figure 4: Computation of the sectorial coordinate ω.

With the aim of defining the equations which govern the structural behaviour of thin-walled open profiles, it is assumed that the beam is subjected to some torsional deformations. As a result of these, each point of the section is characterised by a new position in the general coordinate system XYZ. Therefore, it behaves as a perfectly rigid body, whose position can be evaluated by means of three independent variables corresponding to the three generalized displacements of an arbitrarily chosen point: two translations ξ and η in the X and Y directions, respectively, and the rotation ϑ.

The transverse displacements ξ and η of any point belonging to the cross section can be determined through the well-known expressions:

$$u = \xi(z) - \vartheta(z)\, y \tag{20a}$$

$$v = \eta(z) + \vartheta(z)\, x \tag{20b}$$

The tangential displacement δ_t, related to the generic point of the section, can be computed by

$$\delta_t = \{\delta\}^T \{u_t\} = u\frac{dx}{ds} + v\frac{dy}{ds} \tag{21}$$

and then:

$$\delta_t = \xi\frac{dx}{ds} + \eta\frac{dy}{ds} + \vartheta h(s) \tag{22}$$

in which the term $h(s)$ represents the distance between origin of the reference system and tangent line to the section midline (Figure 4):

$$h(s) = \{r\}^T \{u_n\} = x\frac{dy}{ds} - y\frac{dx}{ds} \tag{23}$$

The longitudinal displacement component w can be obtained by the second Vlasov's hypothesis, according to which the shearing strains on the midline are considered negligible:

$$\gamma_{zs} = \frac{\partial w}{\partial s} + \frac{\partial \delta_t}{\partial z} = 0 \tag{24}$$

Taking into account the following relationship

$$\omega(s) = \int_0^s h(s)\, ds \tag{25}$$

the analytical expression of w is derived by integration,

$$w = \zeta(z) - \int_0^s \frac{\partial \delta_t}{\partial z} ds = \zeta(z) - \xi' x - \eta' y - \vartheta' \omega \tag{26}$$

The term $\zeta(z)$ is an arbitrary function, depending only on z, which describes a longitudinal translation of the entire section; $\omega(s)$ is the **sectorial area**, i.e. the double of the area swept by the radius vector $\{r\}$ from $s = 0$ to the current point s of the section's midline. The points O and $s = 0$ are the **sectorial pole** and the **sectorial origin**, respectively (Figure 4).

The longitudinal component w is composed by four terms: the first three are well-known and arise from extension and bending in the XZ and YZ planes. The component which describes the warping of the section is expressed by the fourth term and, in particular, ϑ' can be considered as an amplification factor, whereas ω as the shape of the warped section.

By differentiating w with respect to z, it is possible to obtain the expression of the longitudinal deformation ε_z:

$$\varepsilon_z = \frac{\partial w}{\partial z} = \zeta' - \xi'' x - \eta'' y - \vartheta'' \omega \tag{27}$$

The fourth term of Equation (27) demonstrates that the hypothesis of primary torsion, according to which the unit angle of torsion should be constant, in general can be removed.

The general expression of the normal stresses is obtained multiplying Equation (27) by the elastic modulus E:

$$\sigma_z = E\left(\zeta' - \xi'' x - \eta'' y - \vartheta'' \omega\right) \tag{28}$$

In each section of the beam, the normal stress σ_z is the sum of two contributions:

$$\sigma_z = \sigma_z^{SV} + \sigma_z^{VL} \tag{29}$$

where:

$$\sigma_z^{VL} = -E\vartheta'' \omega \tag{30}$$

This expressions demonstrate that normal stresses can appear not only in presence of uniform extension and bending of the beam, but also as a result of the non-uniform torsion of the cross section. On the other hand, this specific contribution is usually assumed to vanish in the theory of primary torsion.

The computation of the sectorial terms is carried out considering the origin of the generic right-handed system XYZ as sectorial pole and a generic sectorial origin on the midline (Figure 5), the expression (28) allows to define, by integration, the normal stress acting along cantilever:

$$N = \int_A \sigma_z dA = E\left(A\zeta' - S_y \xi'' - S_x \eta'' - S_\omega \vartheta''\right) \tag{31}$$

Supposing null the axial force in the vertical bracing, the term ζ' can be eliminated in Equation (31):

$$\zeta' = \frac{S_y}{A}\xi'' + \frac{S_x}{A}\eta'' + \frac{S_\omega}{A}\vartheta'' = x_G \xi'' + y_G \eta'' + \omega_0 \vartheta'' \tag{32}$$

The substitution of Equation (32) into Equation (28) permits to define the internal actions related to the flexural behaviour of the beam:

$$M_y = \int_A \sigma_z x dA = -E\left(J_{yy}\xi'' + J_{yx}\eta'' + J_{y\omega}\vartheta''\right) \tag{33a}$$

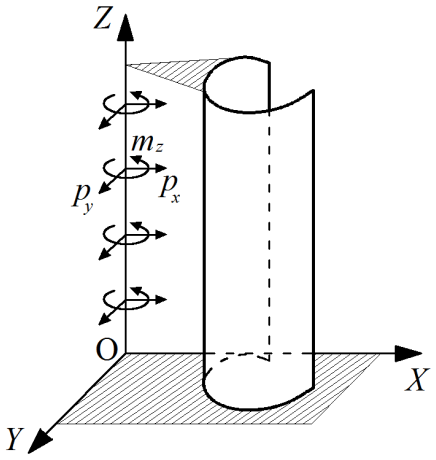

Figure 5: Thin-walled open-section beam subjected to transversal actions.

$$M_x = \int_A \sigma_z y dA = -E\left(J_{xy}\xi'' + J_{xx}\eta'' + J_{x\omega}\vartheta''\right) \tag{33b}$$

$$B = \int_A \sigma_z \omega dA = -E\left(J_{\omega y}\xi'' + J_{\omega x}\eta'' + J_{\omega\omega}\vartheta''\right) \tag{33c}$$

where:

$$J_{yy} = I_{yy} - Ax_G^2 \tag{34a}$$

$$J_{xx} = I_{xx} - Ay_G^2 \tag{34b}$$

$$J_{xy} = I_{xy} - Ax_G y_G \tag{34c}$$

$$J_{\omega\omega} = I_{\omega\omega} - A\omega_0^2 \tag{35a}$$

$$J_{\omega y} = I_{\omega y} - A\omega_0 x_G \tag{35b}$$

$$J_{\omega x} = I_{\omega x} - A\omega_0 y_G \tag{35c}$$

Equation (33c) defines the bimoment action, which represents a generalized self-balanced force system equivalent to two bending moments, having the same magnitude but opposite signs.

Equations (34) represent the implementation of Huygens-Steiner theorem, which transfers the system XYZ from the generic origin to the centroid of the section. Similarly, Equations (35) express the sectorial properties, being the sectorial pole unvaried.

It is possible to write these terms in a compact form introducing the matrix of inertia [*J*]:

$$[J] = \begin{bmatrix} J_{yy} & J_{yx} & J_{y\omega} \\ J_{xy} & J_{xx} & J_{x\omega} \\ J_{\omega y} & J_{\omega x} & J_{\omega\omega} \end{bmatrix} \tag{36}$$

The tangential stresses τ_{zs}, supposed to be defined by a constant distribution on the thickness of the section, can be obtained considering the longitudinal equilibrium of an elementary portion of beam, whose dimensions are the length d*z*, the width d*s*, and the thickness *b* (Figure 6):

$$\frac{\partial(\tau_{zs}b)}{\partial s} + \frac{\partial(\sigma_z b)}{\partial z} = 0 \tag{37}$$

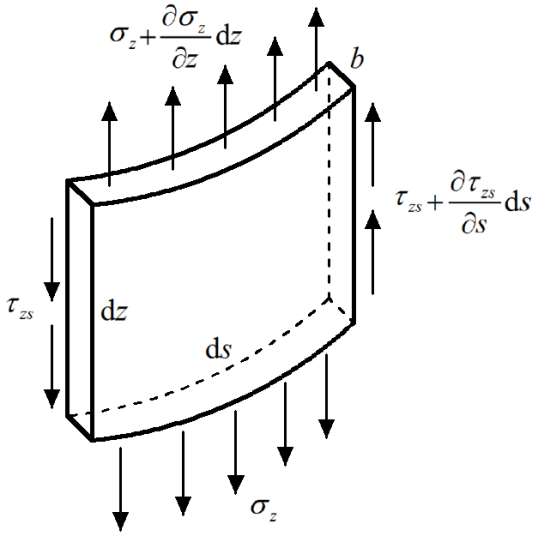

Figure 6: Longitudinal equilibrium of an infinitesimal strip of beam.

On the basis of Equation (37), three additional transverse internal actions, the shearing forces and the secondary torsional moment, can be defined:

$$T_x = \int_A \tau_{zs} \frac{dx}{ds} dA \tag{38a}$$

$$T_y = \int_A \tau_{zs} \frac{dy}{ds} dA \tag{38b}$$

$$M_z^{VL} = \int_A \tau_{zs} h dA \tag{38c}$$

Integrating by parts and applying Equation (37), the following relations are obtained:

$$T_x = -\int_C \frac{\partial(\tau_{zs}b)}{\partial s} x ds = \int_C \frac{\partial(\sigma_z b)}{\partial z} x ds = \frac{d}{dz}\int_A \sigma_z x dA \tag{39a}$$

$$T_y = -\int_C \frac{\partial(\tau_{zs}b)}{\partial s} y ds = \int_C \frac{\partial(\sigma_z b)}{\partial z} y ds = \frac{d}{dz}\int_A \sigma_z y dA \tag{39b}$$

$$M_z^{VL} = -\int_C \frac{\partial(\tau_{zs}b)}{\partial s} \omega ds = \int_C \frac{\partial(\sigma_z b)}{\partial z} \omega ds = \frac{d}{dz}\int_A \sigma_z \omega dA \tag{39c}$$

Disregarding the torsional rigidity GI_t, the Equations (34) and (35) also affect the system (39), which becomes:

$$T_x = \frac{dM_y}{dz} = -E\left(J_{yy}\xi''' + J_{yx}\eta''' + J_{y\omega}\vartheta'''\right) \tag{40a}$$

$$T_y = \frac{dM_x}{dz} = -E\left(J_{xy}\xi''' + J_{xx}\eta''' + J_{x\omega}\vartheta'''\right) \tag{40b}$$

$$M_z^{VL} = \frac{dB}{dz} = -E\left(J_{\omega y}\xi''' + J_{\omega x}\eta''' + J_{\omega\omega}\vartheta'''\right) \tag{40c}$$

The last equation highlights that, due to the warping of the section, an unexpected torsional moment M_z^{VL} is generated, being it the first derivative of the bimoment action.

The secondary torsional moment M_z^{VL} is generated by the τ_{zs} stresses due to the shearing actions T_x and T_y.

A further step of differentiation leads to the equilibrium equations which take into account the distributed external loads p_x, p_y, and m_z (known terms):

$$p_x = -\frac{dT_x}{dz} = E\left(J_{yy}\xi^{IV} + J_{yx}\eta^{IV} + J_{y\omega}\vartheta^{IV}\right) \tag{41a}$$

$$p_y = -\frac{dT_y}{dz} = E\left(J_{xy}\xi^{IV} + J_{xx}\eta^{IV} + J_{x\omega}\vartheta^{IV}\right) \tag{41b}$$

$$m_z = -\frac{dM_z^{VL}}{dz} = E\left(J_{\omega y}\xi^{IV} + J_{\omega x}\eta^{IV} + J_{\omega\omega}\vartheta^{IV}\right) \tag{41c}$$

Actually, the thin-walled open section is subjected to two different torsional moments: the first, due to a constant distribution of tangential stresses through the thickness, is related to the equilibrium with the normal stresses coming from the warping of the section; the second, according to Saint Venant's theory, is due to a linear variation of tangential stresses through the thickness and is equal to zero on the midline.

In each section of the beam, the torsional moment M_z is the sum of the two contributions:

$$M_z = M_z^{SV} + M_z^{VL} = GI_t\vartheta' - E\left(J_{\omega y}\xi''' + J_{\omega x}\eta''' + J_{\omega\omega}\vartheta'''\right) \tag{42}$$

and, therefore, the global equilibrium Equation (41c) becomes:

$$m_z = -\frac{dM_z}{dz} = -\frac{dM_z^{SV}}{dz} - \frac{dM_z^{VL}}{dz} = -GI_t\vartheta'' + E\left(J_{\omega y}\xi^{IV} + J_{\omega x}\eta^{IV} + J_{\omega\omega}\vartheta^{IV}\right) \tag{43}$$

where G is the shear modulus and I_t is the torsional stiffness factor of the section.

If the vectors $\{\delta\}$, $\{M\}$, $\{T\}$, and $\{F\}$ are introduced,

$$\{\delta\} = \begin{Bmatrix} \xi \\ \eta \\ \vartheta \end{Bmatrix} \tag{44a}$$

$$\{M\} = \begin{Bmatrix} M_y \\ M_x \\ B \end{Bmatrix} \tag{44b}$$

$$\{T\} = \begin{Bmatrix} T_x \\ T_y \\ M_z^{VL} \end{Bmatrix} \tag{44c}$$

$$\{F\} = \begin{Bmatrix} p_x \\ p_y \\ m_z \end{Bmatrix} \tag{44d}$$

it is possible to write systems (33), (40), and (41) in a compact form:

$$\{M\} = -E\,[J]\left\{\delta''\right\} \tag{45a}$$

$$\{T\} = -E\,[J]\left\{\delta'''\right\} \tag{45b}$$

$$\{F\} = E\,[J]\left\{\delta^{IV}\right\} \tag{45c}$$

The system of Equations (45) can be strongly simplified operating some choices. In fact, if a centroidal coordinate system is considered, the following conditions are all immediately satisfied:

$$S_y = \int_A x dA = 0 \tag{46a}$$

$$S_x = \int_A y dA = 0 \tag{46b}$$

In addition, if the reference system is also principal, the product of inertia are null

$$J_{xy} = J_{yx} = \int_A xy dA = 0 \tag{47}$$

On the other hand, if the sectorial pole coincides with the shear centre of the section, it can be shown that:

$$J_{\omega y} = J_{y\omega} = \int_A \omega x dA = 0 \tag{48a}$$

$$J_{\omega x} = J_{x\omega} = \int_A \omega y dA = 0 \tag{48b}$$

In addition, if the sectorial origin is in the sectorial centroid, by definition it follows that also the sectorial static moment is null

$$S_\omega = \int_A \omega dA = 0 \tag{49}$$

When centroid and shear centre do not coincide, the diagonalization of the Vlasov's equations, namely, of the relationship between the diagonal terms of matrix [J] and the second derivatives of the generalized displacements, is possible only in the case $N = 0$.

If each of this hypothesis is satisfied, it is possible diagonalized the matrix [J]:

$$[J] = \begin{bmatrix} J_{yy} & 0 & 0 \\ 0 & J_{xx} & 0 \\ 0 & 0 & J_{\omega\omega} \end{bmatrix} \tag{50}$$

Taking into account this diagonal matrix, the Equations (45) can be written in simplified form and the internal actions can be defined as:

$$M_y = -EJ_{yy}\xi'' \tag{51a}$$

$$M_x = -EJ_{xx}\eta'' \tag{51b}$$

$$B = -EJ_{\omega_C\omega_C}\vartheta'' \tag{51c}$$

The internal actions producing the tangential stresses are also diagonalized:

$$T_x = -EJ_{yy}\xi''' \tag{52a}$$

$$T_y = -EJ_{xx}\eta''' \tag{52b}$$

$$M_z^{VL} = -EJ_{\omega_C\omega_C}\vartheta''' \tag{52c}$$

This means that the system of Equations (41) is reduced to the following decoupled equilibrium equations:

$$p_x = EJ_{yy}\xi^{IV} \tag{53a}$$

$$p_y = EJ_{xx}\eta^{IV} \tag{53b}$$

$$m_z = EJ_{\omega_C\omega_C}\vartheta^{IV} - GI_t\vartheta'' \tag{53c}$$

Imposing the boundary conditions, the system can be solved and functions ξ, η, and, ϑ can be determined together with the normal and tangential stresses.

It is interesting to observe that Equation (53c) is formally the same as the equation of the elastic line with effects of the second order due to a tensile axial load N:

$$q(z) = EIv^{IV} - Nv'' \tag{54}$$

It is worthwhile to emphasize the formal analogy between the well-known equations of the elastic line describing the flexural behaviour of a beam and the diagonalized differential equations describing the torsional behaviour of thin-walled open-section beams.

As in the case of flexural curvature, in the torsional behaviour the term ϑ'' vanishes where the bimoment is null, or, in other words, the bimoment is zero where the line describing the rotations of the beam shows an inflection point.

If the contribution related to the primary torsion $GI_t\vartheta''$ is negligible, Equation (53c) can be more easily integrated.

Since the matrix of inertia is symmetrical and positive definite until the geometry of the section is such that the determinant of $[J]$ is different from zero, it can be inverted in order to obtain a relationship between the fourth derivatives of the displacements and the external distributed actions:

$$\left\{\delta^{IV}\right\} = \frac{1}{E}[J]^{-1}\{F\} \tag{55}$$

The transverse displacements of the section are obtained integrating Equation (55) and applying the boundary conditions at the base and at the top of the cantilever.

At the constrained end:

$$\{\delta\} = \{0\}, \quad \{\delta'\} = \{0\}, \quad \text{for} \quad z = 0 \tag{56a,b}$$

whereas, at the top:

$$\{\delta''\} = \{0\}, \quad \{\delta'''\} = \{0\}, \quad \text{for} \quad z = l \tag{57a,b}$$

Once ξ, η, and ϑ are known, the application of Equation (32) yields the uniform axial displacement ζ with the corresponding boundary condition:

$$\zeta(z = 0) = 0 \tag{58}$$

Eventually, the displacement components δ_t and w can be easily derived from Equations (22) and (26).

This analytical formulation cannot be applied in presence of specific sections for which the matrix $[J]$ is singular. These are the cases of shear walls constituted by a single thin rectangular plate or different thin plates converging into a single point, as shown in Figure 7. In these cases the warping function vanishes.

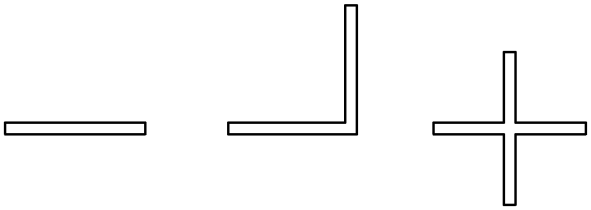

Figure 7: Shear walls constituted by thin plates converging in a single point.

The previous formulation was extended by Capurso [6] to consider the case of M vertical cantilevers which represent the resistant skeleton of a tall building loaded by transverse actions applied to the floors with reference to the global coordinate system XYZ. The vertical bracings are connected to each other by means of in-plane rigid slabs, whose out-of-plane rigidity can be considered negligible. The unknown variables of the problem are the floor displacements, identified by the translations ξ and η in the X and Y directions, respectively, and the torsional rotation ϑ. If $\{F_i\}$ indicates the vector of the transverse actions transmitted to the i-th cantilever, by virtue of Equation (45c) we have:

$$\{F_i\} = E[J_i]\left\{\delta^{IV}\right\} \tag{59}$$

where matrix $[J_i]$ contains the moments of inertia referred to the centroid of the section and to the sectorial centroid, whereas the vector $\{\delta^{IV}\}$ gathers the derivatives of the fourth order of the floor displacements ξ, η, and ϑ.

If $\{F\}$ is the vector of the external loads, the equilibrium condition imposes:

$$\{F\} = \sum_{i=1}^{M}\{F_i\} = E\left(\sum_{i=1}^{M}[J_i]\right)\left\{\delta^{IV}\right\} = E[J]\left\{\delta^{IV}\right\} \tag{60}$$

Therefore, the combination of M cantilevers behaves as a single cantilever whose matrix of inertia is given by the sum of the M matrices related to the single cantilevers:

$$[J] = \sum_{i=1}^{M}[J_i] \tag{61}$$

Equation (60) can be solved following the procedure previously described in the case of a single vertical bracing. Once the floor displacements are known, the displacements of each cantilever can be deduced and information regarding the stress state can also be obtained. Finally, it is interesting to observe, from the relation between the vector $\{F_i\}$ of the i-th cantilever and the global vector $\{F\}$,

that each bracing is subjected to an external load vector provided by the product of its own inertia matrix by the inverse of the global one, analogously to what emerges in the General Algorithm of Section 2:

$$\{F_i\} = [J_i]\,[J]^{-1}\,\{F\} \tag{62}$$

In the case of a discrete distribution of transverse forces corresponding to the different floors, the 3×3 matrix $[J]$, which is a function of the longitudinal coordinate z, can be expanded to a $3N \times 3N$ stiffness matrix to be inserted in the General Algorithm.

Finally it is possible know the normal stress based on the corresponding internal actions substituting the Equations (51) into Equation (28):

$$\sigma_z = \frac{M_y}{J_{yy}}x + \frac{M_x}{J_{xx}}y + \frac{B}{J_{\omega_C\omega_C}}\omega \tag{63}$$

The first two contributions derive from the well-known Saint Venant's theory and are based on the hypothesis of plane sections; the third describes the normal stresses due to the out-of-plane warping of the profile.

An expression of the tangential stresses τ_{zs} can be obtained substituting Equation (28) into Equation (37)

$$\frac{\partial(\tau_{zs}b)}{\partial s} + Eb\left(\zeta'' - \xi'''x - \eta'''y - \vartheta'''\omega\right) = 0 \tag{64}$$

and integrating with respect to s:

$$\tau_{zs} = -\frac{E}{b}\left[\zeta''A(s) - \xi'''S_y(s) - \eta'''S_x(s) - \vartheta'''S_\omega(s)\right] \tag{65}$$

where the following geometrical expressions are used:

$$A(s) = \int_0^s b\,ds \tag{66a}$$

$$S_y(s) = \int_0^s xb\,ds \tag{66b}$$

$$S_x(s) = \int_0^s yb\,ds \tag{66c}$$

$$S_\omega(s) = \int_0^s \omega b\,ds \tag{66d}$$

The substitution of Equations (52) into Equation (65) gives an expression for the tangential stresses

$$\tau_{zs} = \frac{1}{b}\left[\frac{T_x}{J_{yy}}S_y(s) + \frac{T_y}{J_{xx}}S_x(s) + \frac{M_z^{VL}}{J_{\omega_C\omega_C}}S_\omega(s)\right] \tag{67}$$

The first two terms derive from Jourawski's theory, whereas the last from Vlasov's theory.

4 Dynamic analysis of tall buildings

It is well-known that the higher the building, the more sensitive it becomes to the dynamic actions coming from wind and earthquakes. In the stage of conceptual design, the need of a preliminary assessment of the free vibration frequencies is essential.

Since only mode shapes and natural frequencies will be evaluated, neither external actions will be taken into account, nor forced ground motion is included in the analysis.

Due to D'Alembert's Principle, the inertial forces of the structure can be reduced to static forces and, therefore, included into Equation (16). In particular, the masses of the building floors, together with the corresponding accelerations, appear in the global equilibrium equations. On the other hand, the mass corresponding to the vertical elements is considered negligible and its effect is omitted. As a consequence, the load vector is represented in this case by the product of a mass matrix by a vector containing the inertial accelerations of the building storeys.

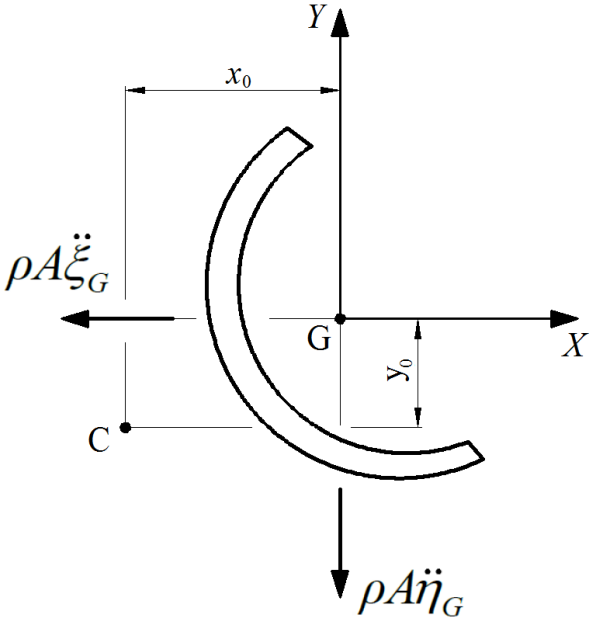

Figure 8: Scheme of the j-th floor of a tall building subjected to inertial forces.

The inertial forces are (Figure 8):

$$p_x = -\rho A\ddot{\xi}_G \tag{68a}$$

$$p_y = -\rho A\ddot{\eta}_G \tag{68b}$$

Let the shear centre C be the origin of the local coordinate system; the transverse displacements of the centroid can be written in terms of the global floor displacements ξ, η, and ϑ through the following expressions:

$$\ddot{\xi}_G = \frac{d^2}{dt^2}(\xi - y_0\vartheta) \tag{69a}$$

$$\ddot{\eta}_G = \frac{d^2}{dt^2}(\eta + x_0\vartheta) \tag{69b}$$

where x_0 and y_0 define the position of centroid with respect to the shear centre.

The actions described by Equations (68), applied in the centroid of the section, produce a torsional moment with respect to the shear centre

$$m_z = -\rho J_p \frac{d^2\vartheta}{dt^2} + \left[\rho A \frac{d^2}{dt^2}(\xi - y_0\vartheta)\right] y_0 - \left[\rho A \frac{d^2}{dt^2}(\eta + x_0\vartheta)\right] x_0 \tag{70}$$

where J_p is the polar moment of inertia of the section referred to the centroid of the section.

Substituting Equations (68) and (70) into Equations (53) yields:

$$EJ_{yy}\frac{\partial^4\xi}{\partial z^4} + \rho A \frac{\partial^2}{\partial t^2}(\xi - y_0\vartheta) = 0 \tag{71a}$$

$$EJ_{xx}\frac{\partial^4\eta}{\partial z^4} + \rho A \frac{\partial^2}{\partial t^2}(\eta - x_0\vartheta) = 0 \tag{71b}$$

$$EJ_{\omega\omega}\frac{\partial^4\vartheta}{\partial z^4} - GI_t\frac{\partial^2\vartheta}{\partial z^2} + \rho J_p\frac{\partial^2\vartheta}{\partial t^2} - \rho A y_0\frac{\partial^2\xi}{\partial t^2} + \rho A y_0^2\frac{\partial^2\vartheta}{\partial t^2} + \rho A x_0\frac{\partial^2\eta}{\partial t^2} + \rho A x_0^2\frac{\partial^2\vartheta}{\partial t^2} = 0 \tag{71c}$$

Using the relationship between the polar moment of inertia referred to the shear center I_0 and that referred to the center of gravity J_p

$$J_p = I_0 - Ay_0^2 - Ax_0^2 \tag{72}$$

and substituting this equation into Equation (71c):

$$EJ_{\omega\omega}\frac{\partial^4\vartheta}{\partial z^4} - GI_t\frac{\partial^2\vartheta}{\partial z^2} + \rho I_0\frac{\partial^2\vartheta}{\partial t^2} - \rho A y_0\frac{\partial^2\xi}{\partial t^2} + \rho A x_0\frac{\partial^2\eta}{\partial t^2} = 0 \tag{73}$$

In general, the three equations are coupled to each other. Only in the case of double symmetry the bending problem is decoupled from the torsion problem.

It is possible to separate the spatial problem from the temporal expressing the unknowns ξ, η, and ϑ as the product of a spatial function $Z(z)$ and a time function $T(t)$

$$\xi = U(z)\,T(t) \tag{74a}$$

$$\eta = V(z)\,T(t) \tag{74b}$$

$$\vartheta = \Theta(z)\,T(t) \tag{74c}$$

Substituting Equations (74) into Equations (71a, 71b) and (73) yields:

$$\frac{EJ_{yy}U^{IV}}{(-\rho AU + \rho A y_0\Theta)} = \frac{\ddot{T}}{T} = -\omega_n^2 \tag{75a}$$

$$\frac{EJ_{xx}V^{IV}}{(\rho AV + \rho A x_0\Theta)} = \frac{\ddot{T}}{T} = -\omega_n^2 \tag{75b}$$

$$\frac{EJ_{\omega\omega}\Theta^{IV} - GI_t\Theta''}{(-\rho I_0\Theta + \rho A y_0 U - \rho A x_0 V)} = \frac{\ddot{T}}{T} = -\omega_n^2 \tag{75c}$$

where ω_n^2 is the square of the angular frequency.

From the system of Equations (75) it is possible to obtain the time-dependent differential equation:

$$\ddot{T} + \omega_n^2 T = 0 \tag{76}$$

The general integral of this equation is given by:

$$T(t) = A_n \cos\omega_n^2 t + B_n \sin\omega_n^2 t \tag{77}$$

The coefficients A_n and B_n can be obtained from the initial conditions of the problem.

Any vibrational motion of the beam can be described as a superposition effect of the mode shapes:

$$\xi = \sum_{n=1}^{\infty} U_n(z)\,T_n(t) \tag{78a}$$

$$\eta = \sum_{n=1}^{\infty} V_n(z)\,T_n(t) \tag{78b}$$

$$\vartheta = \sum_{n=1}^{\infty} \Theta_n(z)\,T_n(t) \tag{78c}$$

The boundary conditions at the constraint ($z = 0$) are:

$$U = V = \Theta = U' = V' = \Theta' = 0 \tag{79}$$

whilst at the top:

$$U'' = V'' = \Theta'' = U''' = V''' = GI_t\Theta' - EJ_{\omega\omega}\Theta''' = 0 \tag{80}$$

The inertial forces are evaluated as the product of the mass matrix of the floors by the vector containing the accelerations of the same floors in the directions X and Y.

Once obtained the vector of displacements $\{\delta\}$ of the floors, it is possible to calculate the displacements of the i-th element and, therefore, the stresses acting on it.

5 Numerical example

A numerical example referred to the case of thin-walled closed- and open-section shear walls is considered. The open sections are analyzed according to the theory of sectorial areas proposed by Vlasov – Capurso.

The matrix formulation proposed in Section 2 for three-dimensional problems proves to be a general approach, which can be easily adapted to every case concerning a system of in-parallel members subjected to transverse actions. Indeed, if the stiffness matrix $[K_i^\star]$ of the i-th element in its own coordinate system is known (Equation (12)), it is possible to implement the formulation in presence of any type of bracing.

With the aim of highlighting the potentiality of the method, a specific numerical example is proposed regarding a 40-storey building, which is 160 m tall and subjected to horizontal forces $F_X = 120$ kN and torsional moments $M_z = 1800$ kNm, applied at each floor level in the origin of the global coordinate system (Figure 9). The cantilevers are made of concrete, whose elastic modulus and Poisson ratio are 3×10^4 MPa and 0.18, respectively.

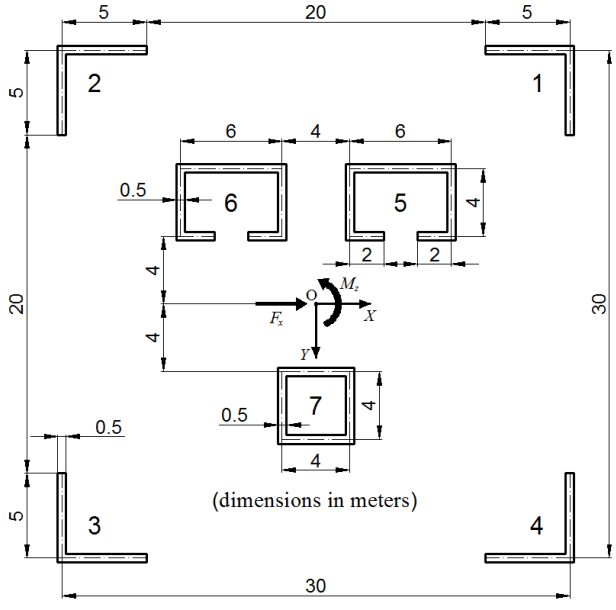

Figure 9: Floor plan of the structure.

The innermost elements exhibit a square hollow closed section and two thin-walled open sections, whereas the perimeter elements are L-shaped open-sections. The static analysis results are shown in Figures 10 and 11, whereas the dynamic analysis outcomes are represented in Figure 12.

In particular, Figure 10(a) shows the transverse displacement $\xi(z)$ in the X direction and its successive derivatives. While the $\xi'(z)$ function represents the slope of the elastic line, the derivatives $\xi''(z)$, $\xi'''(z)$, and $\xi^{IV}(z)$, as shown in Equations (51a), (52a), and (53a), are proportional to the bending moment, the shearing force, and the distributed load, respectively. On the other hand, the values of the global internal actions, $M_y(z)$ and $T_x(z)$, and those of the uniformly distributed load $p_x(z)$, are represented in Figure 10(b).

The transverse displacement in the Y direction, $\eta(z)$, is null, and so are the stresses $M_x(z)$ and $T_y(z)$, and the uniformly distributed load $p_y(z)$ assessed on the equivalent cantilever, as proportional to the subsequent derivatives $\eta(z)$.

Figure 11(a) shows the torsional rotation $\vartheta(z)$ of each floor, and its successive derivatives. Considering the trends of the diagrams, it can be seen that the inflection point in the $\vartheta(z)$ function for $z \cong 65$ m corresponds to a stationary point in the $\vartheta'(z)$ function, and to a zero value of the $\vartheta''(z)$ function at the same level. Similarly, the $\vartheta'(z)$ function presents an inflection point for $z \cong 116$ m, corresponding to a stationary point in the $\vartheta''(z)$ function, and to a zero value of the $\vartheta'''(z)$ function. The $\vartheta'(z)$ function also turns out to be null for $z = 0$. As a matter of fact, the structure is constrained at the base and, in agreement with Equation (26), warping is prevented. In the first three diagrams of Figure 11(b), the values of the primary torsional moment $M_z^{SV}(z)$, of the bimoment action $B(z)$, and of the secondary torsional moment $M_z^{VL}(z)$ are represented. As shown in Equation (42), the primary torsional moment $M_z^{SV}(z)$, and the secondary torsional moment $M_z^{VL}(z)$ result to be proportional to $\vartheta'(z)$ and $\vartheta'''(z)$, respectively, while the bimoment $B(z)$ is proportional to $\vartheta''(z)$, as proved by Equation (42). In the fourth diagram of Figure 11(b), the sum of the moments $M_z^{SV}(z)$ and $M_z^{VL}(z)$ is reported. It is to be noted that the secondary torsional moment is one order of magnitude lower than the primary torsional moment.

As regards the dynamic analysis, the first six mode shapes and the corresponding natural frequencies are shown in Figure 12. Generally, in such irregular buildings, the vibration modes are characterized by coupled bending and twisting motions.

In the first three vibration modes do not appear nodal sections in the deformed shape, whereas, in the following three vibration modes, they manifest themselves. In particular, as can be observed in Figure 12, the first modal shape is a prevailing bending along the Y axis, the second one is a prevailing torsion along the Z axis, while the third mode is predominantly torsional. The fourth and fifth shapes are coupled bending-torsional modes, and present

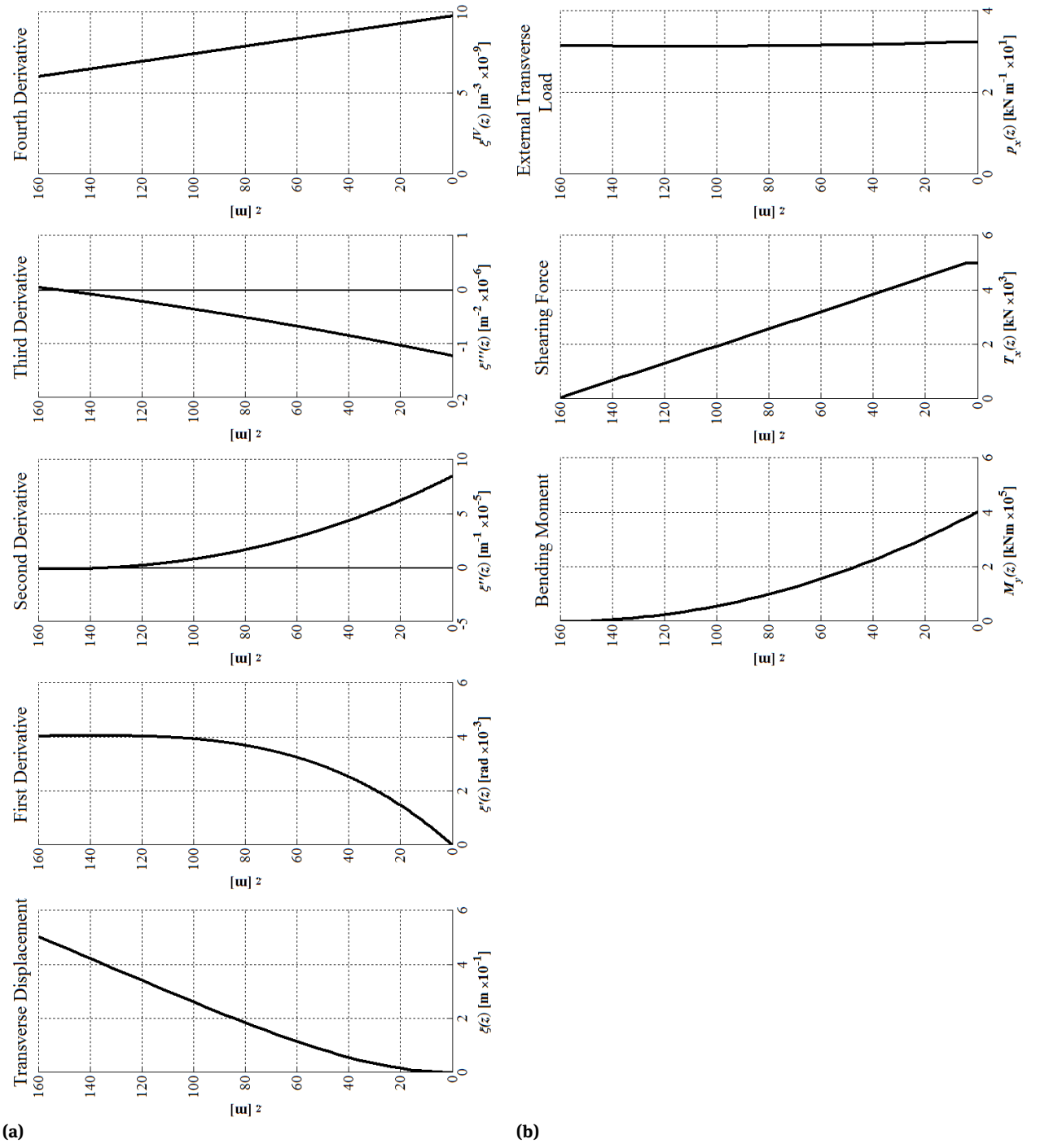

Figure 10: (a) Transverse displacement $\xi(z)$ in the X direction and its successive derivatives; (b) Global internal actions $M_y(z)$ and $T_x(z)$, and those distributed load $p_x(z)$.

one nodal section. In the former case, the bending occurs mainly along the Y axis, whereas in the latter it occurs prevailingly in the X direction. Finally, the sixth mode shape is predominantly torsional, and presents two nodal sections, as shown in Figure 12.

Figure 13(a,b) show the first ten periods and frequencies of the structure vibrations modes. The mode of vibration with the longest period (and consequently the lowest frequency) is termed fundamental mode. The other modes with shorter period of vibration are termed higher modes.

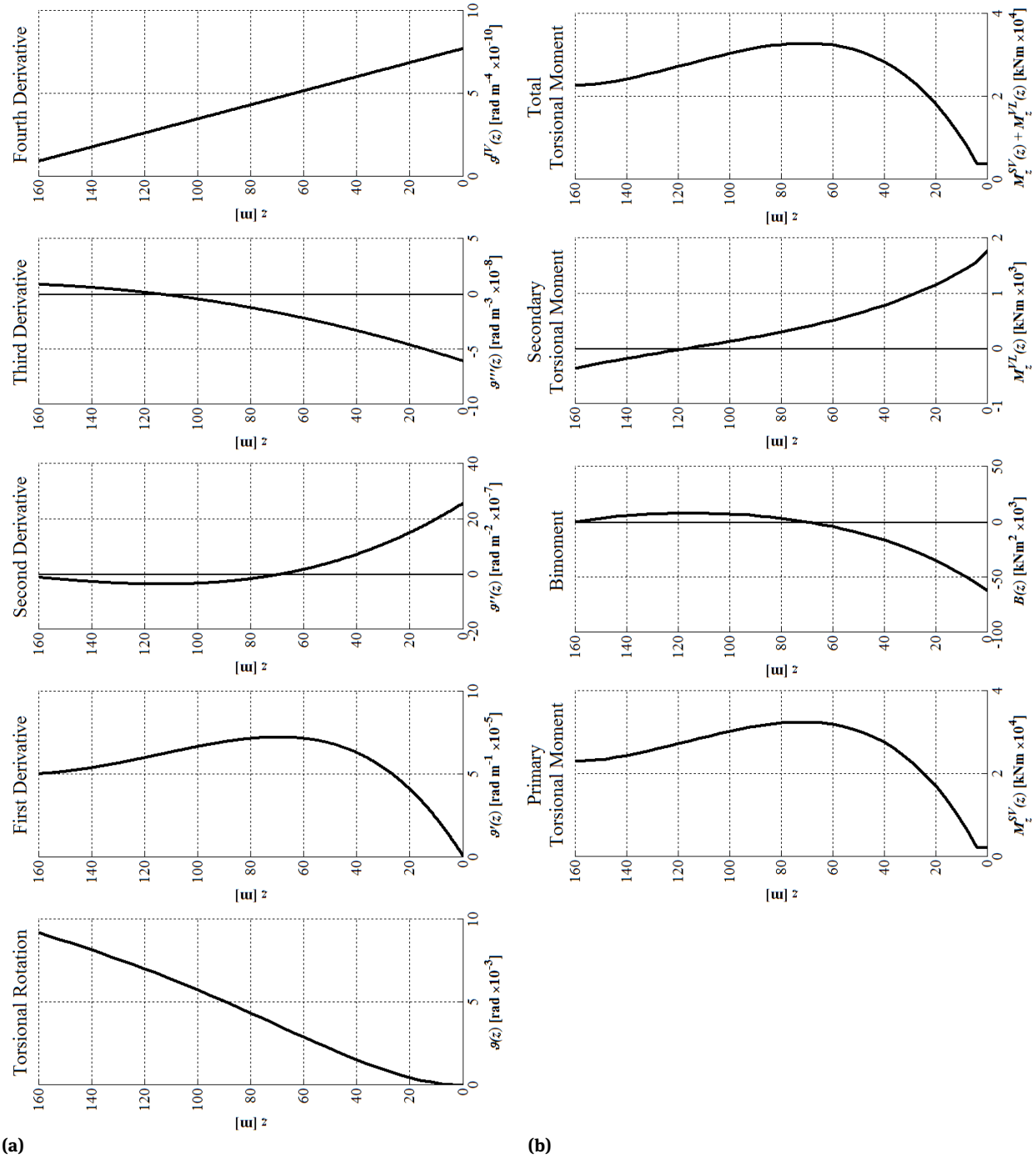

Figure 11: (a) Torsional rotation $\vartheta(z)$ of each floor and its successive derivatives; (b) Global internal actions $M_z^{SV}(z)$, $B(z)$, and $M_z^{VL}(z)$.

It is noted that the first mode of vibration has its own period of approximately 10 seconds. This value is very high if compared to an ordinary structure, but it is an usual value for a tall building. Considering that the fundamental period of an earthquake is about 1 second, it can be deduced that tall buildings are poorly susceptible to the resonance effects due to the earthquakes, and consequently the most significant effects are due to the wind induced loads.

Moreover, the stress distribution of the open shear-wall no. 6 has been analysed; its geometry is shown in Figure 14. The calculation was carried out at the base of the building ($z = 0$), in the discrete points defined in Figure 14.

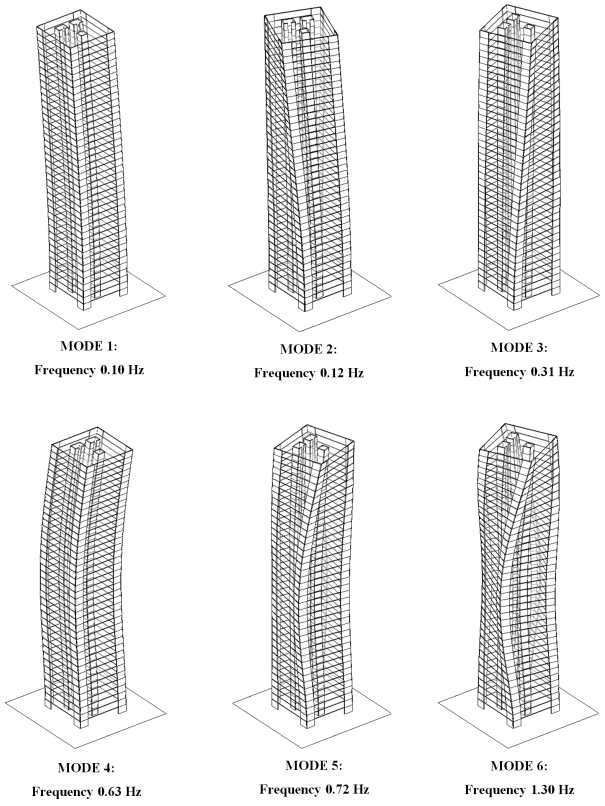

Figure 12: The first six mode shapes and the corresponding natural frequencies.

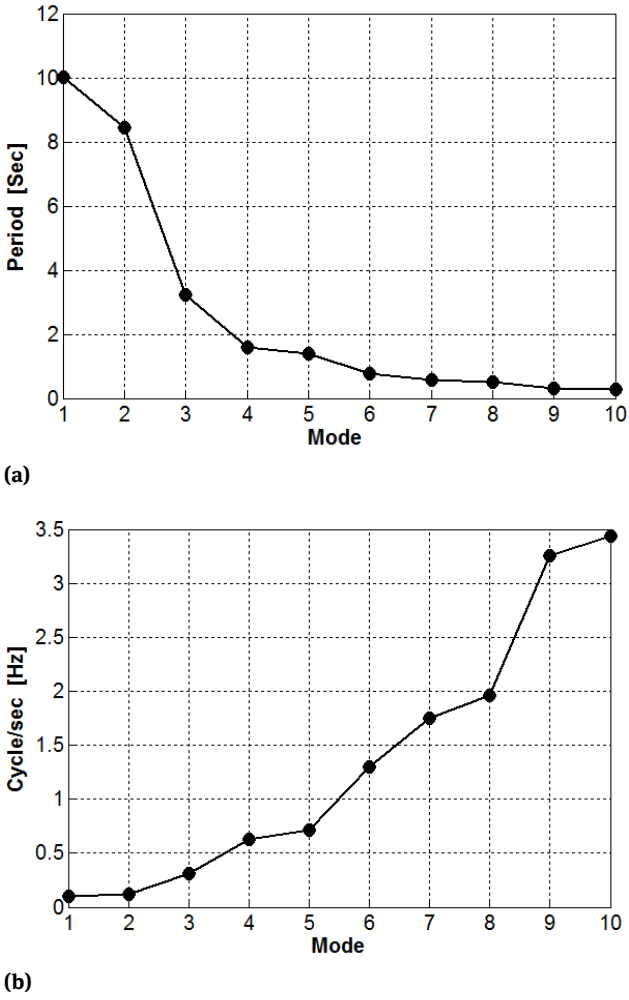

Figure 13: (a) The first ten periods of vibration of the structure; (b) The first ten frequencies of vibration of the structure.

Once the position of the element's shear centre has been determined in relation to the global reference system, the Equation (63) allows to calculate the axial stresses produced by the horizontal loads, and the Equation (67) allows to calculate the shearing stresses due to shearing forces.

Figure 15 shows the trend of axial stresses calculated according to Saint Venant's, taking into account the bending moments, and to Vlasov's theory, considering the bimoment (see Equation (63)). In the diagram, the values $\sigma_z = \sigma_z^{SV}$ and $\sigma_z = \sigma_z^{SV} + \sigma_z^{VL}$ are quoted. The figure shows that the contribution of the bimoment σ_z^{VL} leads to a 10% variation of stress produced by the flexure σ_z^{SV}.

If the contribution of the normal stress due to the dead loads is also considered, σ_z^G, the diagram represented in Figure 16 is obtained. From the diagram it can be seen that, in this particular case, the stress contribution due to the dead loads, σ_z^G, is comparable to that generated by bending moments and bimoment, $\sigma_z = \sigma_z^{SV} + \sigma_z^{VL}$. While, on the basis of previous analyses performed by the authors, it is shown how in high-rise structures generally the normal stresses due to horizontal loads exceed by about 80% the dead load stresses. Moreover, it is interesting to note as in ordinary buildings the contribution of normal stresses due the dead loads is generally prevalent if compared to that generated by the lateral forces.

As for the calculation of shearing stresses shown in Figure 17 (see Equation (67)), the effect of the secondary torsional moment, $\tau_{zs}^{VL} = \frac{1}{b}\left[\frac{M_z^{VL}}{J_{\omega_C\omega_C}} S_\omega(s)\right]$ adds a significant increment of more than 50% on average, to shearing stresses caused by the shearing forces, $\tau_{zs}^{SV} = \frac{1}{b}\left[\frac{T_x}{J_{yy}} S_y(s) + \frac{T_y}{J_{xx}} S_x(s)\right]$, throughout the whole plan development of the section.

6 Conclusions

In the present paper, a three-dimensional formulation is proposed, which evaluates the structural behaviour of

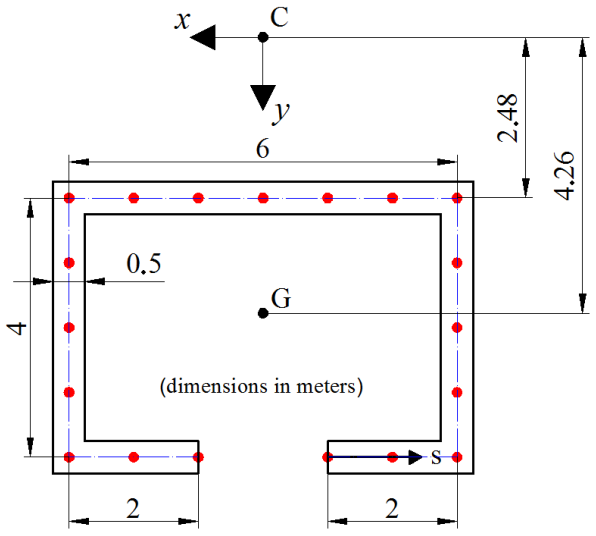

Figure 14: Dimensions of the open shear-wall no. 6.

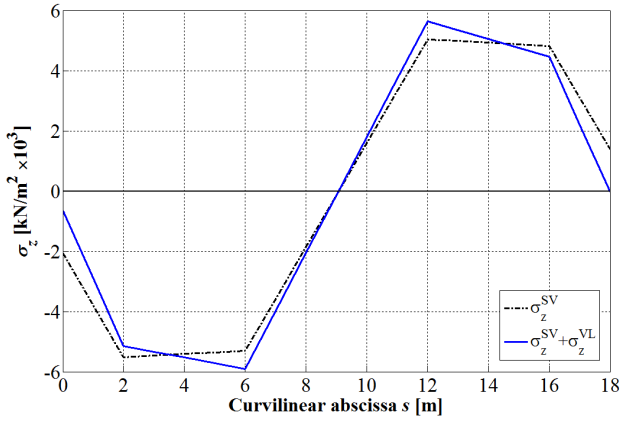

Figure 15: Axial stresses due to horizontal loads acting on open shear wall no. 6.

high-rise buildings stiffened by open and closed shear-walls.

Although being dependent on some simplifying hypotheses, as specified in Section 2, this analytical calculation method allows to achieve solutions in a shorter time and with a lower memory usage, if compared to FEM modelling. The analytical model has always three degrees of freedom for each storey, whilst the FEM approach, which is mesh-dependent, is characterised by six degrees of freedom for each node. As for the computation accuracy, studies carried out on real structures [30] show that the maximum difference between the analytical and the FEM displacement calculation is around 15–20%.

This difference is usually accepted during the preliminary design when the general analysis of the problem is

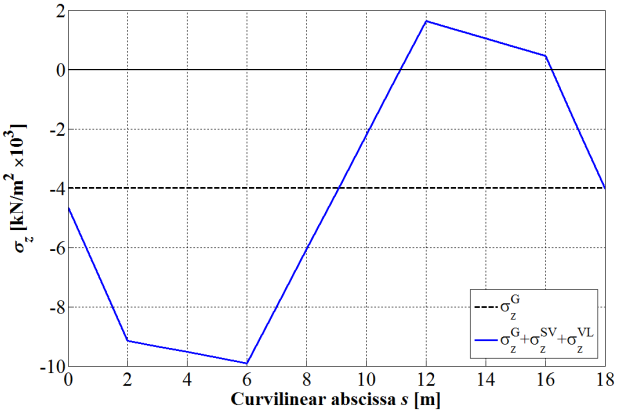

Figure 16: Axial stresses due to horizontal and dead loads acting on open shear wall no. 6.

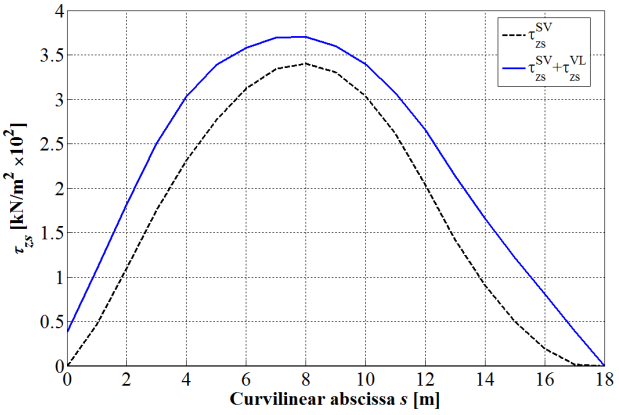

Figure 17: Tangential stresses acting on open shear wall no. 6.

preferred, as in these phases loads are usually overestimated and materials' resistances are underestimated.

In the numerical example and according to the results contained in Section 5, the ability is shown of the analytic formulation to capture the main information regarding the static and dynamic behaviour of a tall building subjected to lateral forces. The transverse displacements as well as the distribution of the external actions between the vertical members constituting the whole resistant system are, in fact, crucial for the necessary preliminary analysis.

References

[1] V. Vlasov, Thin Walled Elastic Beams (2nd ed.), Jerusalem: Israeli Program for scientific translation, US Science Foundation, Washington, 1961

[2] H. Wagner, W. Pretschner, Torsion and buckling of open sections, NACA Tech. Mem. N.784 (1936)

[3] S.T. Timoshenko, Theory of bending, torsion and buckling of thin walled members of open section, Journal of the Franklin In-

stitute, 239, N. 3,4,5 (1945)
[4] T. Von Karman, C. Wei-Zang, Torsion with variable twist, Journal of the Aeronautical Science, 13, 503, (1946)
[5] M. Capurso, Sul calcolo delle travi in parete sottile in presenza di forze e distorsioni, La ricerca Scientifica, 6, (1964), 213–241 (in Italian)
[6] M. Capurso, Sul calcolo dei sistemi spaziali di controventamento, Giornale del Genio Civile, 1–2–3, (1981), 27–42 (in Italian)
[7] A. Carpinteri, An. Carpinteri, Lateral loading distribution between the elements of a three-dimensional civil structure, Computers and Structures 2, (1985), 563–580
[8] S. Timoshenko, Theory of Elastic Stability (1st ed.), McGraw-Hill Book Company Inc., New York, 1936
[9] B.S. Taranath, Structural Analysis and Design of Tall Buildings: Steel and Composite Construction, CRC Press, New York, 2011
[10] W.P. Howson, Global analysis: Back to the future, The Structural Engineer 84 (2006), 18–21
[11] R.D.J.M. Steenbergen, J. Blaauwendraad, Closed-form super element method for tall buildings of irregular geometry, International Journal of Solids and Structures 44 (2007), 5576–5597
[12] F.R. Khan, J.A. Sbarounis, Interaction of shear walls and frames, Journal of the Structural Division, Proceedings of ASCE, 90 ST3, (1964), 285–335
[13] A. Coull, A.W Irwin, Analysis of load distribution in multi-storey shear wall structures, Structural Engineering, 48, (1970), 201–306
[14] A.C. Heidebrecht, B. Stafford Smith, Approximate analysis of tall wall-frame structures, Journal of the Structural Division, ASCE, 99, (1973), 199–221
[15] A. Rutenberg, A.C. Heidebrecht, Approximate analysis of asymmetric wall-frame structures, Building Science, 10, (1975), 27–35
[16] F.K.E.C. Mortelmans, G.P.J.M. De Roeck, D.A. Van Gemert, Approximate method for lateral load analysis of high-rise buildings, Journal of the Structural Division, ASCE, 107, (1981), 1589–1610
[17] F.R. Khan, Tubular structures for tall buildings, Handbook of Concrete Engineering, Van Nostrand Reinhold Co, New York, 1974
[18] A. Coull, B. Bose, Simplified Analysis of Frame – Tube Structures, Journal of the Structural Division, ASCE, 101-11, (1975), 2223–2240
[19] J.J. Connor, C.C. Pouangare, Simple model for design of framed tube structures, Journal of Structural Engineering, ASCE, 117, (1991), 3623–3644
[20] A.K.H. Kwan, Simple Method for Approximate Analysis of Framed Tube Structures, Journal of Structural Engineering, ASCE, 120-4, (1994), 1221–1239
[21] R. Rahgozar, A. R. Ahmadi, M. Ghelichi, Y. Goudarzi, M. Malekinejad, P. Rahgozar, Parametric stress distribution and displacement functions for tall buildings under lateral loads, Structural design of tall and special buildings, 23, (2014), 22–41
[22] J. Lee, M. Bang, J.Y. Kim, An analytical model for high-rise wall-frame structures with outriggers, The Structural Design of *Tall* and Special Buildings, 17, (2008), 839–851
[23] J.C.D. Hoenderkamp, H. Snijder, Approximate analysis of high-rise frames with flexible connections, The Structural Design of *Tall* and Special Buildings, 9, (2000), 233–248
[24] H.S. Kim, D.G.Lee, Analysis of shear wall with openings using super elements, Engineering Structures, 25, (2003), 981–991
[25] S.A. Meftah, A. Tounsi, A.B. El-Abbas, A simplified approach for seismic calculation of a tall building braced by shear walls and thin-walled open section structures, Engineering Structures, 29, (2007), 2576–2585
[26] X.Z. Lu, L.L. Xie, C. Yu, X. Lu, Development and application of a simplified model for the design of a super-tall mega-braced frame-core tube building, Engineering Structures, 110, (2016), 116–126
[27] X.Z. Lu, L.L. Xie, H. Guan, Y.L. Huang, X. Lu, A shear wall element for nonlinear seismic analysis of super-tall buildings using OpenSees, Finite Elements in Analysis and Design, 98, (2015), 14–25
[28] A. Carpinteri, G. Lacidogna, S. Puzzi, A global approach for three dimensional analysis of tall buildings, The Structural Design of Tall and Special Buildings 19 (2010), 518–536
[29] A. Carpinteri, M. Corrado, G. Lacidogna, S. Cammarano, Lateral load effects on tall shear wall structures of different height, Structural Engineering and Mechanics 41, (2012), 313–337
[30] A. Carpinteri, G. Lacidogna, S. Cammarano, Structural analysis of high-rise buildings under horizontal loads: A study on the Intesa Sanpaolo Tower in Turin, Engineering Structures, 56, (2013), 1362–1371
[31] A. Carpinteri, G. Lacidogna, S. Cammarano, Conceptual design of tall and unconventionally shaped structures: A handy analytical method, Advances in Structural Engineering 17, (2014), 757–773
[32] A. Carpinteri, A., G. Lacidogna, B. Montrucchio, S. Cammarano, The effect of the warping deformation on the structural behaviour of thin-walled open section shear walls, Thin-Walled Structures, 84, (2014), 335–343